Identifying salmon lice transmission characteristics between Faroese salmon farms

Kragesteen, Trondur J.; Simonsen, Knud; Visser, AW; Andersen, Ken Haste

Published in:
Aquaculture Environment Interactions

Link to article, DOI:
10.3354/aei00252

Publication date:
2018

Document Version
Peer reviewed version

Identifying Salmon Lice Transmission Characteristics between Faroese Salmon Farms

Tróndur J. Kragesteen[1,2], Knud Simonsen[1], André W. Visser[2], and Ken H. Andersen[2]

[1]Fiskaaling - Aquaculture Research Station of the Faroes, við Áir 11, FO430 Hvalvík, Faroe Islands

[2]VKR Centre for Ocean Life, National Institute of Aquatic Resources, Technical University of Denmark, Building 202, 2800 Kgs. Lyngby, Denmark

November 24, 2017

Abstract

Sea lice infestations are an increasing challenge in the ever-growing salmon aquaculture sector and cause large economic losses. The high salmon production in a small area creates a perfect habitat for parasites. Knowledge of how salmon lice planktonic larvae disperse and spread the infection between farms is of vital importance in developing treatment management plans to combat salmon lice infestations. Using a particle tracking model forced by tidal currents, we show that Faroese aquaculture farms form a complex network. In some cases as high as 10% of infectious salmon lice released at one farm site enter a neighboring fjord containing another farm site. Farms were characterize as emitters, receivers or isolated, and we could identify two clusters of farms that were largely isolated from each other. The farm characteristics are a valuable input for the development of management plans for the entire Faroese salmon industry.

Running page head: Salmon Lice Transmission Characteristics between Faroese Salmon Farms

KEY WORDS: Connectivity, Dispersal, Tidal Forcing, Particle Tracking, Salmon lice.

INTRODUCTION

In salmonid aquaculture, the infestation of parasitic organisms is a major challenge and causing significantly economic losses in the aquaculture industry. The treatment cost are estimated to be around € 0.25/kg (Costello 2009) and applied on the global salmon production in 2015 of 2.3 million tonnes (FAO 2017) the sea lice management cost translates to roughly € 575 million. The estimated treatment cost per kg, although widely used may be outdated (Shinn et al. 2015). In addition, the parasites impacts the global aquaculture industry with negative publicity (Adams et al. 2015) due to the possible damage the parasite has on the environment as a result of chemical treatments and it's influence on local wild life (Ford & Myers 2008). Consequently, salmon lice are a major obstacle in any further expansion of the salmon aquaculture industry.

As in other temperate coastal areas, the production of Atlantic salmon in the Faroe Islands has expanded to become a major activity. With an annual production now exceeding 80,000 ton the Faroe Islands is currently the fifth largest salmon producing country, and the aquaculture industry has become a major economic player locally as it accounts for 46% of the Faroese export value in 2016 (SFI 2017). In 2014 the cost of drugs to combat sea lice used by the Faroese salmon farming industry exceeded € 18 million, or roughly € 0.22/kg. Introduction of cleaner fish and mechanical treatments has however reduced the expenses of chemoterapeutants to less than € 13 million in 2016 (SFI 2017).

Sea lice is a common name for a range of marine ectoparasitic copepods belonging to the family Caligidae. Two sea lice species cause by far the greatest challenge in salmonid aquaculture in the northern hemisphere: *Lepeophtheirus salmonis* and *Caligus elongatus*. *L. salmonis* is a parasite only found on salmonids, often referred to as salmon lice, while *C. elongatus* is a more opportunistic parasite, and has been found on 80 different fish species (Kabata 1979). Of the two species *L. salmonis* has by far the largest economic impact on the salmonid aquaculture industry due to its damaging effect on its host (Boxaspen 2006).

The increased salmon production has elevated the density of the naturally occurring salmon lice in the water column primarily due to the large growth in the number of hosts. The high density further increases the chances of transmitting salmon lice between hydrodynamically connected farms. Additionally, experience shows that sporadic uncontrolled treatment of salmon lice in an area yields a resistant salmon lice population over time (Murray 2011, Aaen et al. 2015). Farms with intense

treatment might quickly develop resistant salmon lice strains. In inter-connected farm networks the resistant strains spread out to the whole network after a given period. Therefore, in connected farm networks, there may be a point when the external infection pressure reaches a stage when, from a farmers perspective, treatment becomes virtually pointless. Coordinated treatment management plans are thus essential to achieve long term sustainable control of salmon lice. Achieving control requires a thorough understanding of the sea lice dispersion patterns, a factor highly dependent on regional and local hydrography (Adams et al. 2015).

Dispersion of salmon lice larvae has been studied using numerical models in Scotland (Amundrud & Murray 2009, Adams et al. 2012, Salama et al. 2013, Adams et al. 2015), Canada (Stucchi et al. 2011) and Norway (Asplin et al. 2014, Johnsen et al. 2014, 2016, Samsing et al. 2017). For a more comprehensive overview, see Salama & Rabe (2013). In some fjord systems farms were found to be inter-connected (Adams et al. 2012, Johnsen et al. 2016), while in other cases several clusters of connected farms could be identified (Salama et al. 2013, 2017). Samsing et al., (2017) investigated the connectivity between most farms on the Norwegian cost and found seasonal variations to influence the connectivity. These cases needs different management strategies, emphasizing the importance of knowing the specific farm network. This study presents a first attempt to investigate the dispersion of salmon lice and connectivity between aquaculture farms in the Faroe Islands. While earlier studies have either been on farms located in a restricted area mainly enclosed by land (Adams et al. 2012, Salama et al. 2013, 2017) or along a long coast with complicated fjord systems (Stucchi et al. 2011, Asplin et al. 2014, Johnsen et al. 2014, 2016, Samsing et al. 2017), this study is of a spatially limited archipelago with a relatively high farm density in a tidal energetic area surrounded by open ocean. The limited number of farms in a nearly isolated system makes Faroe Islands an ideal area to investigate the interaction and population dynamics of salmon lice.

METHODS

Study Area

The Faroe Islands is an archipelago in the Atlantic ocean containing complicated coastlines, multiple fjords and connecting straits (Fig. 1). The distance from the northernmost to the southernmost point is about 110 km. Due to its location in the path of the North Atlantic Current the sea around Faroe Island is dominated by relatively warm and saline waters with fairly stable conditions. The temperature varies from 6°C in February to approximately 10°C in August and September and the variation in salinity is confined to 35.05–35.25 ‰ on the shelf (Larsen et al. 2008, Gaard et al. 2011), but is seen reduced towards 32‰ in the fjords due to freshwater runoff (Gaard et al. 2011).

The waters on the Faroe Shelf can be characterized as a tidal energetic system, although the tidal elevation amplitude is quite modest. The amplitude of the dominating M_2-constituent varies from some 60 cm in the westernmost islands to less than 10 cm at the central eastern coast (Simonsen & Niclasen 2011), which may be characterized as a semi-amphidromic point. This relatively large gradient towards the central east coast creates strong currents with maximum speeds up to 3.6 m/s (Fig. 1) in some straits (Larsen et al. 2008, Simonsen & Niclasen 2011). Further, Larsen et al., (2008) showes that the tides through rectification are the main driver of a steady current clockwise around the islands (Fig. 2).

In some of the fjords, and in the strait between the two biggest islands (white arrowhead, Fig. 1), the tides has less influence on the circulation (Fig. 1) and stratification may occur mainly due to the freshwater runoff (Gaard et al. 2011). In these areas, estuarine and wind driven circulation is of significant importance.

Outside the fjords, however, the water masses are quite homogeneous due to the intense mixing caused mainly by tidal currents (Larsen et al. 2008). We therefore focus on the tidal component in the model due to the dominating influence it has on water movement around the Faroe Islands. Including only the tidal component simplifies the model, but still reveals the general background dispersion pattern.

Model Overview

The underlying tidal circulation model is an implementation of the barotropic mode of the Regional Ocean Model System (ROMS) (Shchepetkin & McWilliams 2005) on a half nautical mile grid resolution covering a larger area, and on a 100 m resolution grid for the coastal region (Simonsen & Niclasen 2011). The higher resolution model was forced by the solution from a coarser model, which applied altimetry generated data by Egbert et al., (1994) along its open sea boundaries. After a spin-up period, data were stored at one hour intervals in every grid point in 30 days for tidal analysis using the Ttide software (Pawlowicz et al. 2002). Validation of the derived harmonic constants towards similar data derived from observed timeseries from tidal gauges and current measurement showed a general good agreement (Simonsen & Niclasen 2011). Here the current is estimated from the dominating constituents and the residual current obtained from the 100 m resolution tidal model.

Tidal Current

We included three semi diurnal constituents: M_2, S_2 and N_2, two diurnal constituents: K_1 and O_1, one over-tide constituent M_4, and the residual current. The east (u) and north (v) component of the forcing current at a given time (t) is obtained by summing up the contribution from the six (n) tidal constituents and residual current (u_r, v_r) at each horizontal position (x, y):

$$u(t,x,y) = u_r(x,y) + \sum_i^n a_i(x,y)\cos(\omega_i t - \varphi(x,y))\cos(\theta(x,y)) - b_i(x,y)\sin(\omega_i t - \varphi(x,y))\sin(\theta(x,y)) \tag{1}$$

$$v(t,x,y) = v_r(x,y) + \sum_i^n a_i(x,y)\cos(\omega_i t - \varphi(x,y))\sin(\theta(x,y)) - b_i(x,y)\sin(\omega_i t - \varphi(x,y))\cos(\theta(x,y)) \tag{2}$$

$$\omega_i t = 2\frac{\pi}{T_i}t \tag{3}$$

where φ_i is the Greenwich phase lag, θ_i the inclination and a_i and b_i are the major and minor semi-axis, respectively, defining the tidal ellipse at a given geographical location of the i'th constituent with frequency $\omega_i(t)$ and corresponding period T_i.

Particle Tracking Model

Salmon lice are represented as passive particles, each representing an arbitrary but uniform number of salmon lice. Because the tidal current model is barotropic, the current is assumed to be vertically uniform, and the vertical movement of the salmon lice is omitted. Turbulent diffusion was included with a horizontal random walk component (Visser 1997). The trajectories of each particle is calculated with an Euler scheme where the position (x, y) of particle q at the next time step, $t + \Delta t$, is calculated from the velocity, u and v:

$$x_q(t + \Delta t) = x_q(t) + u(x, y, t)\Delta t + R\sqrt{6D_h\Delta t} \tag{4}$$

$$y_q(t + \Delta t) = y_q(t) + v(x, y, t)\Delta t + R\sqrt{6D_h\Delta t}, \tag{5}$$

where R is a uniformly distributed random number between $[-1, 1]$. D_h is the diffusion coefficient and set to 0.1 m^2/s (Gillibrand & Willis 2007). The computational cheap and easily implemented Euler scheme was chosen instead of a more accurate higher order scheme. This loss of numerical accuracy is justified by the inclusion of the turbulent diffusion term, which anyway leads to diffusion. A sensitivity analysis of the time step was conducted (not shown) and satisfying convergence was obtained with a time step of 0.005 h (18 sec), which is used in the present simulations. Particles crossing the outer boundary are considered lost and removed from the simulation. At the shoreline a no flux reflective boundary condition is applied (Brickman et al. 2009). For the particle tracking simulation the 100 m resolution grid of the tidal model is adopted. The number of particles released was tested and the mean trajectory of the particle cluster between identical simulations was found to be reasonably converged when releasing 900 particles every hour.

Biological Parameters

When modeling the dispersion of salmon lice the three non-feeding planktonic stages, nauplii I, nauplii II and copepodid are relevant. The non-infectious *L. salmonis* napulii larvae hatch from the adult female egg strings and are released into the planktonic environment where they moult into a second nauplii stage and further into the infectious copepodid larvae (Pike & Wadsworth 1999). Being non-feeding, the planktonic larvae have only the energy from their internal yolk reserves for survival and therefore need to locate and infect a host within a limited life span. Infection of a

new host is determined by the survival of the larvae and the likelihood of a infectious larvae making contact with a new host. The infection rate is a function of attachment success, water currents, temperature, salinity, grazing, etc..

In our model salmon lice larva biology is represented by three processes: The duration of the nauplii and copepodid stages and the mortality. The development time of the planktonic phases are primarily determined by the water temperature at salinity above 30 ‰ (Samsing et al. 2016). Here we assume a summer scenario with sea temperature of 10°C. The duration and longevity in these first phases decreases with increasing temperature. Both Johnson & Albright (1991) and Samsing et al. (2016) found a similar development time for *L. salmonis* naupulii, and at 10 °C they spend ≈ 3.7 days to develop into a infectious copepodid, while the longevity of the copepodid at the same temperature is approximately 13 days (Gravil 1996, Samsing et al. 2016).

Determining mortality is harder because studies of *L. salmonis* larvae in their natural environment are scarce. Stien et al., (2005) studied population dynamics of *L. salmonis* and estimated a mortality rate of napulii to be ≈ 0.17 d^{-1} and copepodid to be ≈ 0.22 d^{-1}, based on laboratory experiments. The survival probability over time is:

$$p(t) = e^{-\mu t} \tag{6}$$

where p is the survival probability at time t. Mortality (μ) was assumed to be 0.17 d^{-1} for both planktonic phases.

Naupulii and copepodid larvae have been shown to be photo-tactic as well as having the ability to migrate away from low salinity and seek higher temperature in the upper layers (Johnsen et al. 2014, á Norði et al. 2015, Johnsen et al. 2016). Gillibrand & Willis (2007) and Johnson et al. (2014) showed that relative small vertical movement behaviors had a significant effect on the dispersion pattern in stratified waters emphasizing the need for a more comprehensive model in estuarine driven areas. However, outside the Faroese fjords where the circulation is dominated by the tides (Larsen et al. 2008), the connectivity between the salmon farming locations will those also be dominated by tides.

Simulations and Connectivity Matrices

Based on the existing farm locations as listed by the authorities, 24 farm sites were defined, to which a receiving and an emitting area was assigned (Fig. 3). The emitting area corresponds to the actual farm site locations. In those cases where several farms are located in a fjord only the farm site closest to the fjord opening is included (Fig. 3). The model is barotropic, and thus no attempt is made to simulate the estuarine circulation which may appear in fjords with little tidal influence (Fig. 1). The neglected estuarine circulation is, however, of importance for the dispersion within these fjords, and consequently the receiving farm area (or "hit area") is subjectively defined as the entire fjord if the farm is located inside a fjord or the long narrow strait between the two largest islands (Fig. 3). A copepodid larvae entering these areas is considered an infection risk to the whole area. Farms located in more open and tidal dominated areas (farm 5, 9 and 13, Fig. 3) are assigned a receiving area which corresponds to the farming site. This is different from other connectivity studies where a fixed area around the farm is considered to pose an infectious risk to the farm ranging between a 500 m radius (Adams et al. 2012, Salama et al. 2017) to a 600x600m (Johnsen et al. 2016) and 800x800m area around the farm (Samsing et al. 2017).

The connectivity matrices were generated by releasing 900 particles every hour from each defined farm site emitting area (1.8 million particles) over a period of 2000 hours (83.3 days). The simulation period includes several spring-neap tide cycles and gives the system sufficient time to converge and therefore reflects a long term dispersion trend. All farms are evenly weighted assuming this is a linear process and therefore the exact number of salmon lice a particle represents becomes irrelevant in this context. We adopted a similar approach as described by Adams et al., (2012) where particles can infect any farm, including its initial release farm, when they are older than 3.7 days. Further, the particles have an infections window of 13 days, assuming a typical Faroese summer scenario with 10°C water temperature. A particle was only allowed to infect a given farm site once, meaning that if they re-enter the same farm site the particles were not recorded. However the particle was allowed to continue in the simulation and potentially infect a new farm site, which is different from Adams et al., (2012) where particles were taken out of the simulation when the first connection was made. Particles were taken out of the simulation when they become older than 16.7 days. The connection probability between two farms is calculated as the ratio between infectious particles entering one farm's receiving area from another farm and the total amount of released particles from the emitting

farm. An average age of the infectious particles in a connection is estimated using the age at their entry into a receiving area. The connection probability between two farms including mortality is found by weighing the infectious particles with the survival probability using Eq. 6.

RESULTS

Dispersion

Examples of particle dispersion patterns are illustrated in dispersion maps showing the mean age over the simulation period of particles released from farms 2, 5 and 21 (Fig. 4) in every 100x100m grid cell. The three locations were chosen by their geographic location and because they are placed in tidally relatively exposed areas allowing larvae to escape their initial release site, but at different rates.

Particles disperse rapidly from farm 5 (Fig. 4b), which is located in the energetic strait on the west side of the largest island in the center. In contrast, the particle dispersion from the other two farm sites (Fig. 4a and c) is slow the first couple of days, as seen by the limited dispersal area of the youngest particles (red color). However, once particles escape their initial fjord, they enter what might be called a "dispersion highway", that goes clockwise around the Faroe Islands. Here, they quickly disperse around the archipelago. These results illustrate that larvae are capable of travelling to almost any location around the Faroe Islands, some more likely than others, within their ≈ 2 week lifespan, provided that they manage to escape their release area. Further, the clockwise residual current also implies that only few particles are lost from the system.

The maximum Euclidean distance traveled by a particle varies greatly between farms. Particles can easily travel more than 20 km during the nauplii phase (3.7 days in Faroese summer conditions; Fig. 6a). In three farms, one being farm 5 (dash line with cross), over half of the particles travel over 40 km. On the other hand particles older than 3.7 days generally travel, not surprisingly, significantly longer distances than their nauplii counterparts (Fig. 6b). Here over 50% of particles from most farms travel over 50 km. In several farms, including farms 5 and 21, approximately 10% of the particles travel at least 80 km. It may be noted that the particles are not weighted with mortality here.

The relative distribution of nauplii and copepodid particles in each 100x100m grid cell over the whole simulation period, including mortality, is shown with a heat map (Fig. 5). Here, particles are recorded every time step and weighed with survival probability. Particles released from many farms (10-11 and 22-23) have a very limited dispersion range both in the nauplii and copepodid stage. On the other hand particles released from farms in more exposed areas as farms 5 and 9 have

relativity low densities at their initial release sites, indicating the quick dispersion away from these areas after being released. No clear "cold" spots, i.e. areas with relatively low density of copepodids, are in the coastal regions. The exception is some of the fjords with little tidal influence where estuarine circulation, which is neglected in the present simulation, must be expected to dominate the dispersion (Fig. 5b). The highest density is found around the northern group of islands, which is also where the majority of the farms are located.

Connectivity

The proportion and mean age of infectious salmon lice larvae that disperse between Faroese salmon farms is summarized in three connectivity matrices (Fig. 7). The connectivity matrices reveal generally a high connection between farms although the range of connectivity is quite diverse. The diagonal line indicates the degree of self-infection and is dependant on the strength of exposure in the area. Farm 5, 9, and 13, which are located in tidally exposed areas (Fig. 3), are clearly not self-infectious (Fig. 7a and c). The farms 10-12, 20, 22, and 23 are close to 100% self-infectious and emit very few larvae to other farms, while also having a relatively (to the amount emitted) high infection rate from other farms.

The mean age in the highly self-infectious connections is close to 3.7 days, the time when larvae become infectious, while the mean age for non-self-infectious farms is much higher, between 8-14 days (Fig. 7b). Larvae from farm 5 infecting farm 9 are very old (14-16 days) and vice versa, even though they are very close geographically implying that the particles have traveled a long distance before they enter the neighbour site. Interestingly, however, larvae from these farms infect nearby farms (4, 6, 7 and 8) with younger larvae.

Figure 7c illustrates how infectious a connection is by accounting for mortality. Here the defined receiving area around farm 15 receives over 10% of infectious particles from farm 16, which is the strongest connection in the network. The matrices in figure 7, reveal at least two clusters of farms in the Faroe Islands. One includes farms 1-3, which appear to be internally well connected with quite limited interaction with the other farms. With the exception of a few isolated farms, the rest of the network comprises a large connected cluster.

Farms are characterized as emitters, receivers, and/or isolated by looking at how many infectious larvae they emit and receive to and from other farms, excluding self-infection, expressed as % of

particles corresponding to the amount released from one farm site (Fig. 8). Farms 16, 18, 21 and 14 are the highest emitting, while farm 15 is by far the highest receiving farm followed by farms 5, 9 and 2. Three farms are virtually isolated (10, 12 and 20, Fig. 8), as they are neither receivers nor emitters.

DISCUSSION

Our results demonstrate that Faroese salmon farms form a complex network with a wide range of connectivity strengths. The overall connectivity appears to be much higher than other studies (Adams et al. 2012, 2015, Salama et al. 2013, Johnsen et al. 2016, Salama et al. 2017, Samsing et al. 2017), although a direct comparison is problematic due to the difference in how connectivity is defined. Particles quickly disperse far and wide once outside a fjord and inside the "dispersion highway" which runs clockwise around the Faroe Islands. For the most dynamic sites there is a high probability that the particles reach more than a 20 km distance from their origin, while in the most isolated fjords there is less than 10% probability that the particles travel longer than 20 km before they become infectious. The maximum expected distance in the non-infectious stage is about 60 km for a few sites (Fig. 6a). Including the life span of the copepodid stage there is a fairly high probability for the majority of the sites that the maximum distance is beyond 50 km and some few sites there is up 10% probability that they even reach beyond 80 km (Fig. 6b), which are distances comparable with the geographical size of the archipelago. Note that these distances are maximum Euclidean distances, however, the actually traveled sea distance may be considerable longer as they travel around the islands. Consequently, particles have the potential not only to infect the other farms, but also a potential risk of a delayed self-infection. The presented dispersion distances are comparable with maximum distances found along the Norwegian coast, but considerable longer than the typical 20-40 km found in Norwegian fjords (Asplin et al. 2014) and the median distances of 6 km with maximum distances around 36 km in a Scottish Loch (Salama & Rabe 2013, Salama et al. 2016).

The self-infection in a number of farms is quite high, as seen by the low mean age and small dispersion range in these connections (Fig.'s 7 and 5). The high self-infection is partly caused by the low water fluxes in and out of these fjords, which may be underestimated due to the omission of the estuarine and wind driven circulation, and that the particles stay within the initial receiving area when becoming infections and therefore recorded the moment they become infectious (3.7 days).

Identifying critical nodes in the farm network is highly valuable information when developing a management plan. We were able to identify farms either as emitters, receivers, or isolated. The highest emitting farms (16, 18, 21 and 14, descending order, Fig. 8) are all located in the northern part of the Faroe Islands. They all emit the highest proportion of their infectious salmon lice particles

to the close neighbour, farm 15, which is the highest receiving farm (Fig. 3). Farm 16 emits over 10% of its infectious salmon lice to farm 15, which must be considered a very strong connection. One reason farm 15 is the highest receiver is that the defined receiving area is quite large as this fjord is relatively wide. In addition, the connection to the strait outside this fjord includes a tidally rectified eddy at the fjord mouth, which transports particles into the area. The connection decreases significantly if the receiving line at the fjord mouth is moved further into the fjord. Therefore, care should be taken in drawing too bold conclusions on this relatively strong connection, but still it indicates that the infection risk in this fjord is noticeable. The situation is quite different for the two following farms in the receiving rank list. They both have a modest receiving area, but have a large tidal through-flow resulting in a high particle flux from other farms.

The connectivity matrices suggest that the three farms at the southernmost islands (farms 1-3) are largely separated from the other islands, but are internally well connected. The rest of the farm network seems to be one cluster with negligible contribution from the three isolated farms (10, 12 and 20) and the three relatively isolated farms (11 and 22-23) (Fig. 8). These isolated farms are in the narrow strait between the two main islands and in fjords in the northeast group of islands, which all are characterized by weak tidal currents (Fig. 1). Likely the dispersion within these areas is dominated by estuarine and/or wind driven circulation (Gaard et al. 2011), which is not included in the present model.

Recently, Paturson et al., (2017) assessed variations in salmon lice population dynamics in Faroese farms in relation to the physical exposure to the local circulation patterns and flushing with adjacent waters expressed through an exposure index, and found that up to 65% of the variations in the sea lice dynamics was related to the freshwater input and tides. In the fjords with farms 20 and 22-23, they found a generally low exposure, of which 60-70% was explained by the fresh water runoff, and a general higher exposure index for the fjord hosting farm 10 where nearly 90% of the sea lice variance could be related to the freshwater runoff. A study conducted in Kaldbaks fjord (farm 10, Fig. 3) indicated an average exchange rate of approximately 10 days (Gaard et al. 2011), in contrast to virtually no exchange found in our simulations. Including wind and freshwater forces will increase the interaction with the other farms in the northern cluster as well as the rest of the farm network. However in calm and dry periods, when the tides are the primary forcing mechanism, these farms must be considered as isolated and highly self-infectious.

The connectivity in this study was measured as the number of infectious particles (older than 3.7 days) released at one farm entering the defined receiving area of another farm or its own. Adams et al., (2012) took particles out of the simulation after the first connection. In many cases particles in our simulations did not leave their own receiving area before becoming infectious because we defined the whole fjord to be a potential infectious risk. This is evident when looking at the mean age in most of the self-infection connections (Fig 7b). It would be unpractical in our setup to take most particles out of the simulation after one connection as we would then in most cases only observe self-infection. Therefore particles were allowed to continue in the simulation but they were only allowed to infect once in any given connection. One downside with this method is that relevant information is lost, such as the amount of time an infectious salmon louse spends in a farm area. Johnson et al., (2016) and Samsing et al., (2017) partially solved this by letting salmon lice reinfect a farm site multiple times. Some studies include the biomass and/or salmon lice counts into the farm connectivity (Salama et al. 2017, Samsing et al. 2017). This is especially relevant when studying specific time periods and verifying towards salmon lice counts, which however is not the case in our simulations. Here all farms release an equal amount of particles, which can represent any arbitrary uniform number of salmon lice, which provides the option to include number of salmon lice in a future expansion of the model when number of fish and salmon lice counts data at farm level become available. As mentioned, the connectivity probabilities found in this study are high compared to other studies. This is in part due to the way we define our receiving area, but likely also due to salmon lice having a very high dispersion range in Faroe Islands, in contrast to other areas.

Averaged over several spring-neap tide cycles the only parameters that can change the connectivity are the length of the planktonic phases and the mortality. This study assumed typical Faroese summer conditions. We also ran some simulations in winter conditions were the planktonic phases become longer and observed difference in the connectivity, although the overall connectivity pattern look very similar compared to summer conditions.

The Faroe Islands are notoriously windy, especially in the winter months. The dominating wind direction is southwest, while the less frequent direction is east, but the wind direction and strength is highly variable due to the geographical location of the Faroe Islands in the path of the low pressures crossing the Atlantic (Cappelen & Laursen 1998, Larsen et al. 2008). In the fjords and straits the

wind strength and direction is highly influenced by the surrounding mountains, but currently there is no meteorological data with sufficient high spatial resolution available for the area. Most likely wind affects the dispersion dynamics, especially on short time scales forcing salmon lice larvae out of or into a fjord and outside the fjords wind affects the drifting path. However, due to the variability in the wind forcing it is likely that the overall distribution will be even more smeared out than obtained here from the underlying tidal forcing only, but this still remains to be investigated.

The results presented have many implications which can benefit the Faroese aquaculture industry, where at the moment there is no coordinated treatment management plan based on the underlying hydrographic connectivity between the sites. As mentioned, all farms are weighted equally as we assumed a linear process. The connectivity matrices may therefore be seen as a background or underlying connectivity providing options to include the individual farms sea lice pressure when this information is lifted from its confidentiality.

Our results clearly demonstrate that a holistic treatment plan should be developed as salmon farms are not isolated but connected to each other. Intuitively we would strictly manage the farms that are characterized as emitters to prevent unnecessary external infection pressure on other farms e.g. farms 16, 18 and 21 (if all farms contribute equally). On the contrary, Adams (2015) combined connectivity estimates with a salmon lice population dynamic model by Reive et al., (2005) and found that management was most effective when targeting the highest receiving or influx farms, which is somewhat counter-intuitive. This finding suggests the need to include population dynamics, specifically to examine the network response to different treatment strategies.

In addition to treatment strategies, the approach described here can also aid in the planning of farm locations. For instance salmon farmers can decide to place their farms further out or into the fjord. The trend in the Faroe Islands in resent years has been to place farms further out in the fjord to obtain better growth condition due to higher water exchange, less local bed load and less sea lice self infection. By placing farms further out, as recommended by e.g. Samsing el at. (2015), the connectivity between farms increases. In this way, the benefit to the individual farm increases the challenge for the entire farm network. Also the placement of potential new farm sites is problematic as there are no obvious salmon lice "cold spots" close to Faroese coast (Fig. 5), emphasizing the need for a holistic management approach.

CONCLUSION

In the last decade there has been a gradual increase in the use of numerical models to study the dispersion of *L. salmonis* in all leading Atlantic salmon producing countries and they are now at a state where fairly realistic results can be obtained (Stucchi et al. 2011, Salama & Rabe 2013, Asplin et al. 2014, Johnsen et al. 2016, Samsing et al. 2017, Salama et al. 2017). This study presents the first model which can to a certain degree, realistically simulate the mean dispersion patterns in an archipelago with a circulation dominated by tidal currents. The tidal currents and the residual current due to their highly dominating influence on water currents on the Faroe shelf are the main responsible for the connectivity between farms sites as well as acting as a retention mechanism for the resident sea lice population.

We acknowledge that wind and freshwater forcing, which are not included in the present study, will influence the dispersion dynamics, especially on shorter time scales in the more sheltered fjords. However on longer timescales the highly dominating Faroese tidal forcing will reflect the mean dispersion pattern, enabling valuable insight on the background connection between farms in Faroe Islands.

In summary, the basis is developed to create a robust biophysical model which can help find an optimal treatment and management plan for the Faroese aquaculture industry.

Acknowledgements

This study was financially supported by Danmarks Innovationsfond (Grant No. 5189-00032A) and by Granskingarráðið - Research Council Faroe Islands (Grant No. 0450). We also appreciate the valuable comments from Dr. Nabeil Salama and two anonymous reviewers on earlier version of the manuscript.

References

Aaen, S. M., Helgesen, K. O., Bakke, M. J., Kaur, K., & Horsberg, T. E. (2015). Drug resistance in sea lice: a threat to salmonid aquaculture. *Trends in Parasitology*, *31*(2), 72–81.

Adams, T., Black, K., MacIntyre, C., MacIntyre, I., & Dean, R. (2012). Connectivity modelling and network analysis of sea lice infection in loch fyne, west coast of scotland. *Aquaculture Environment Interactions*, *3*(1), 51.

Adams, T., Proud, R., & Black, K. D. (2015). Connected networks of sea lice populations: dynamics and implications for control. *Aquaculture Environment Interactions*, *6*(3), 273–284.

Amundrud, T., & Murray, A. (2009). Modelling sea lice dispersion under varying environmental forcing in a scottish sea loch. *Journal of fish diseases*, *32*(1), 27–44.

á Norði, G., Simonsen, K., Danielsen, E., Eliasen, K., Mols-Mortensen, A., Christiansen, D., ... Patursson, Ø. (2015). Abundance and distribution of planktonic lepeophtheirus salmonis and caligus elongatus in a fish farming region in the faroe islands. *Aquaculture Environment Interactions*, *7*(1), 15–27.

Asplin, L., Johnsen, I. A., Sandvik, A. D., Albretsen, J., Sundfjord, V., Aure, J., & Boxaspen, K. K. (2014). Dispersion of salmon lice in the hardangerfjord. *Marine Biology Research*, *10*(3), 216–225.

Boxaspen, K. (2006). A review of the biology and genetics of sea lice. *ICES Journal of Marine Science: Journal du Conseil*, *63*(7), 1304–1316.

Brickman, D., Ådlandsvik, B., Thygesen, U., Parada, C., Rose, K., Hermann, A., & Edwards, K. (2009). Particle tracking. In *Manual of recommended practices for modelling physical-biological interactions in fish early-life history* (Vol. 295, pp. 1–111). Copenhagen, Denmark: ICES Cooperative Research Reports.

Cappelen, J., & Laursen, E. V. (1998). *The climate of the faroe islands: With climatological standard normals, 1961-90*. Danish Meteorological Institute.

Costello, M. J. (2009). The global economic cost of sea lice to the salmonid farming industry. *Journal of fish diseases*, *32*(1), 115–118.

Egbert, G. D., Bennett, A. F., & Foreman, M. G. (1994). Topex/poseidon tides estimated using a global inverse model. *Journal of Geophysical Research: Oceans*, *99*(C12), 24821–24852.

FAO. (2017). *Fisheries and aquaculture department [online]. rome.* Retrieved 2017-10-17,

from http://www.fao.org/figis/servlet/SQServlet?file=/work/FIGIS/prod/webapps/figis/temp/hqp_3310080681821032850.xml&outtype=html

Ford, J. S., & Myers, R. A. (2008). A global assessment of salmon aquaculture impacts on wild salmonids. *PLoS Biol*, *6*(2), e33.

Gaard, E., Norði, G. Á., & Simonsen, K. (2011). Environmental effects on phytoplankton production in a northeast atlantic fjord, faroe islands. *Journal of Plankton Research*, *33*(6), 947–959.

Gillibrand, P. A., & Willis, K. J. (2007). Dispersal of sea louse larvae from salmon farms: modelling the influence of environmental conditions and larval behaviour. *Aquatic Biology*, *1*(1), 63–75.

Gravil, H. (1996). *Studies on the biology and ecology of the free swimming larval stages of lepeophtheirus salmonis (kröyer, 1838) and caligus elongatus nordmann, 1832 (copepoda: Caligidae)* (Unpublished doctoral dissertation). University of Stirling.

Johnsen, I. A., Asplin, L., Sandvik, A. D., & Serra-Llinares, R. M. (2016). Salmon lice dispersion in a northern norwegian fjord system and the impact of vertical movements. *Aquaculture Environment Interactions*, *8*, 99–116.

Johnsen, I. A., Fiksen, Ø., Sandvik, A. D., & Asplin, L. (2014). Vertical salmon lice behaviour as a response to environmental conditions and its influence on regional dispersion in a fjord system. *Aquaculture Environment Interactions*.

Johnson, S., & Albright, L. (1991). Development, growth, and survival of lepeophtheirus salmonis (copepoda: Caligidae) under laboratory conditions. *Journal of the Marine Biological Association of the United Kingdom*, *71*(02), 425–436.

Kabata, Z. (1979). *Parasitic copepoda of british fishes*. Ray Society.

Larsen, K. M. H., Hansen, B., & Svendsen, H. (2008). Faroe shelf water. *Continental Shelf Research*, *28*(14), 1754–1768.

Murray, A. G. (2011). A simple model to assess selection for treatment-resistant sea lice. *Ecological modelling*, *222*(11), 1854–1862.

Patursson, E. J., Simonsen, K., Visser, A. W., & Patursson, Ø. (2017). Effect of exposure on salmon lice lepeophtheirus salmonis population dynamics in faroese salmon farms. *Aquaculture Environment Interactions*, *9*, 33–43.

Pawlowicz, R., Beardsley, B., & Lentz, S. (2002). Classical tidal harmonic analysis including error estimates in matlab using t_tide. *Computers & Geosciences*, *28*(8), 929–937.

Pike, A., & Wadsworth, S. (1999). Sealice on salmonids: their biology and control. *Advances in parasitology*, *44*, 233–337.

Revie, C. W., Robbins, C., Gettinby, G., Kelly, L., & Treasurer, J. (2005). A mathematical model of the growth of sea lice, lepeophtheirus salmonis, populations on farmed atlantic salmon, salmo salar l., in scotland and its use in the assessment of treatment strategies. *Journal of fish diseases*, *28*(10), 603–613.

Salama, N., Collins, C., Fraser, J., Dunn, J., Pert, C., Murray, A., & Rabe, B. (2013). Development and assessment of a biophysical dispersal model for sea lice. *Journal of Fish Diseases*, *36*(3), 323–337.

Salama, N., Dale, A., Ivanov, V., Cook, P., Pert, C., Collins, C., & Rabe, B. (2017). Using biological–physical modelling for informing sea lice dispersal in loch linnhe, scotland. *Journal of Fish Diseases*.

Salama, N., Murray, A., & Rabe, B. (2016). Simulated environmental transport distances of lepeophtheirus salmonis in loch linnhe, scotland, for informing aquaculture area management structures. *Journal of fish diseases*, *39*(4), 419–428.

Salama, N., & Rabe, B. (2013). Developing models for investigating the environmental transmission of disease-causing agents within open-cage salmon aquaculture. *Aquaculture Environment Interactions*, *4*(2), 91–115.

Samsing, F., Johnsen, I., Dempster, T., Oppedal, F., & Treml, E. A. (2017). Network analysis reveals strong seasonality in the dispersal of a marine parasite and identifies areas for coordinated management. *Landscape Ecology*, 1–15.

Samsing, F., Oppedal, F., Dalvin, S., Johnsen, I., Vågseth, T., & Dempster, T. (2016). Salmon lice (lepeophtheirus salmonis) development times, body size and reproductive outputs follow universal models of temperature dependence. *Canadian Journal of Fisheries and Aquatic Sciences*(ja).

Samsing, F., Solstorm, D., Oppedal, F., Solstorm, F., & Dempster, T. (2015). Gone with the flow: current velocities mediate parasitic infestation of an aquatic host. *International journal for parasitology*, *45*(8), 559–565.

SFI. (2017). *Statistics faroe islands (statbank)*. Retrieved 2017-10-31, from `http://www.hagstova.fo/en/statbank`

Shchepetkin, A. F., & McWilliams, J. C. (2005). The regional oceanic modeling system (roms): a split-explicit, free-surface, topography-following-coordinate oceanic model. *Ocean Modelling*, *9*(4), 347–404.

Shinn, A., Pratoomyot, J., Bron, J., Paladini, G., Brooker, E. E., & Brooker, A. (2015). Economic costs of protistan and metazoan parasites to global mariculture. *Parasitology*, *142*(1), 196–270.

Simonsen, K., & Niclasen, B. (2011). On the energy potential in the tidal streams of the faroe islands. *Tech Rep NVDrit*, *2011*(1), 33.

Stien, A., Bjørn, P. A., Heuch, P. A., & Elston, D. A. (2005). Population dynamics of salmon lice lepeophtheirus salmonis on atlantic salmon and sea trout. *Marine Ecology Progress Series*, *290*, 263–275.

Stucchi, D. J., Guo, M., Foreman, M. G., Czajko, P., Galbraith, M., Mackas, D. L., & Gillibrand, P. A. (2011). Modelling sea lice production and concentrations in the broughton archipelago, british columbia. *Salmon lice: An integrated approach to understanding parasite abundance and distribution. Oxford, UK: Wiley-Blackwell*.

Visser, A. W. (1997). Using random walk models to simulate the vertical distribution of particles in a turbulent water column. *Marine Ecology Progress Series*, *158*, 275–281.

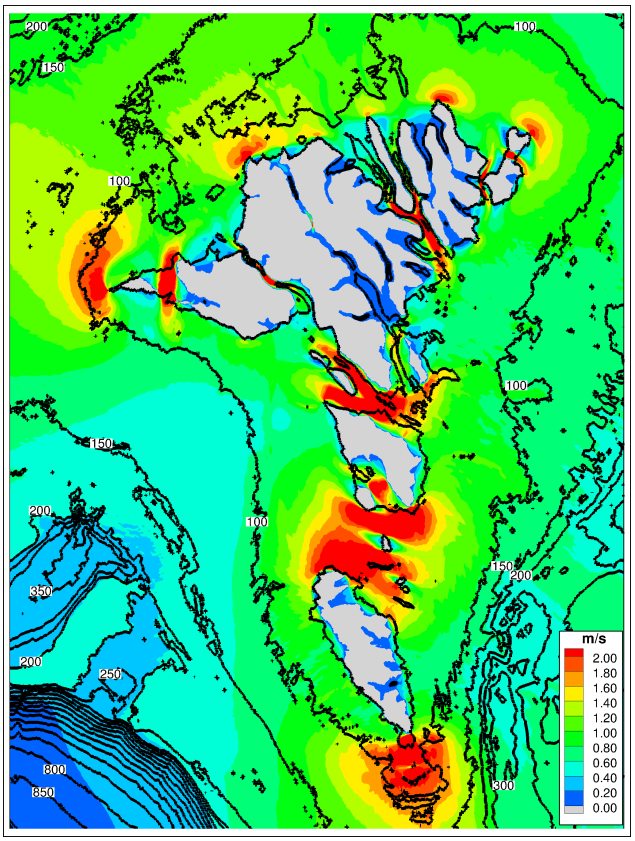

Figure 1: Maximum tidal current velocity provided as the sum of semi-major axis of the 6 dominating constituents (Simonsen & Niclasen, 2011). Thin contour lines provides the water depth. White arrow head shows the location of the large narrow strait.

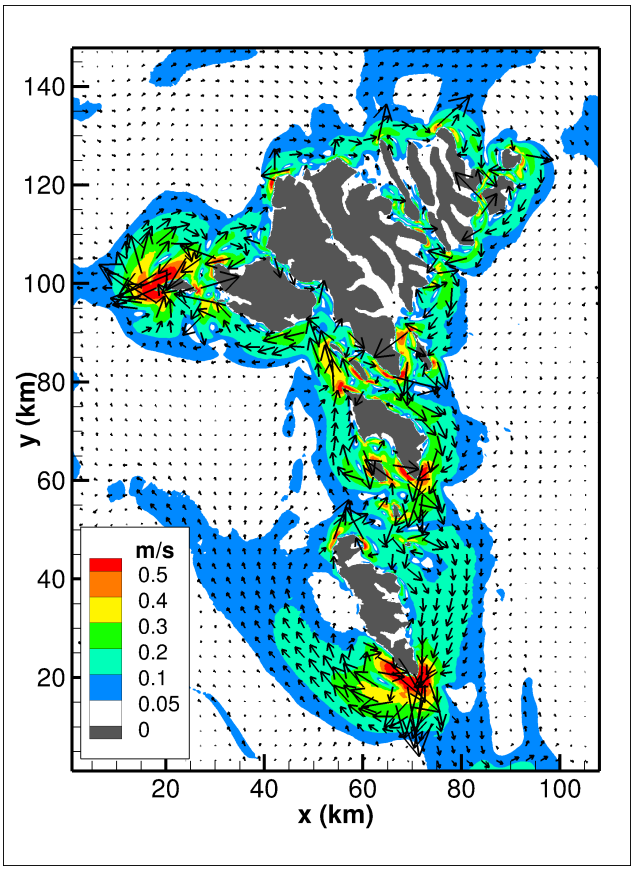

Figure 2: Residual tidal current velocity around the Faroe Islands. The vectors indicate the direction, and the color indicate the speed (Simonsen & Niclasen, 2011). Thin contours lines provides the depth.

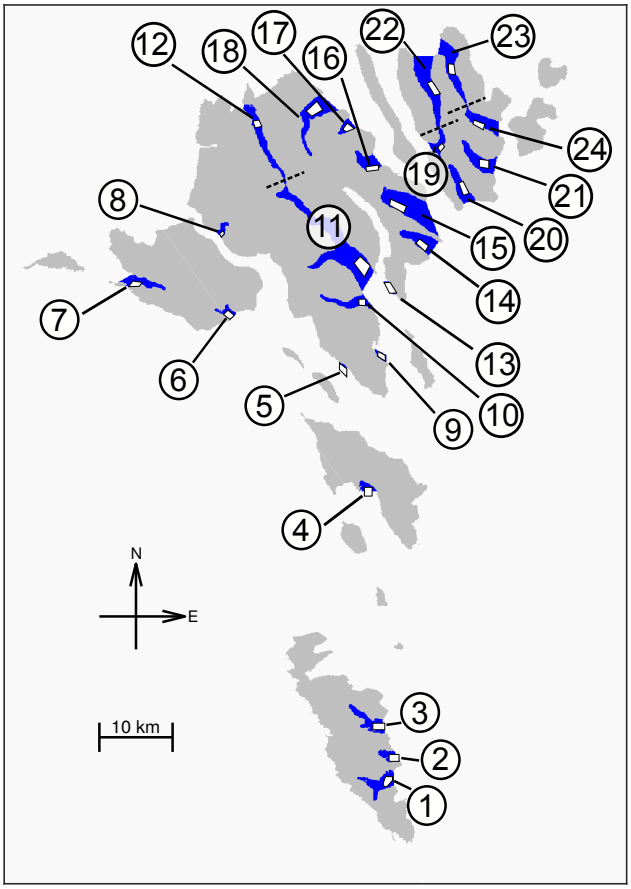

Figure 3: Farm area (blue) and lice release site (white square). Dashed lines distinguishes two farm areas from each other. There is water connection between farm areas 11 and 12, but not between 19 and 22 and 23 and 24.

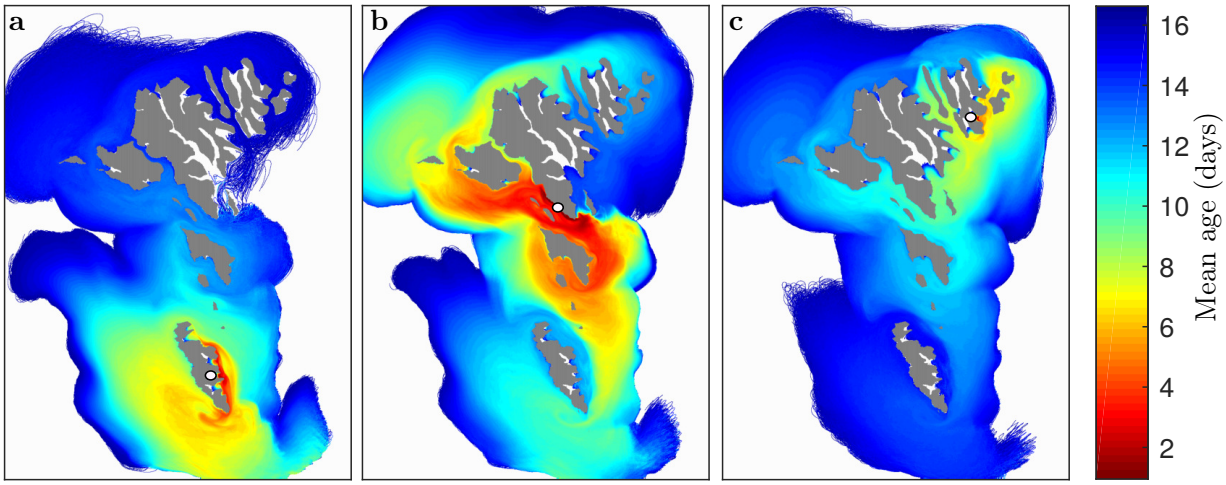

Figure 4: Mean age of particles in every grid cell over the 2000 hour simulation period. 900 particles are released every hour from farm 2, 5 and 21 (white dot) shown in (**a**), (**b**) and (**c**), respectively. Colorbar indicates mean age in days.

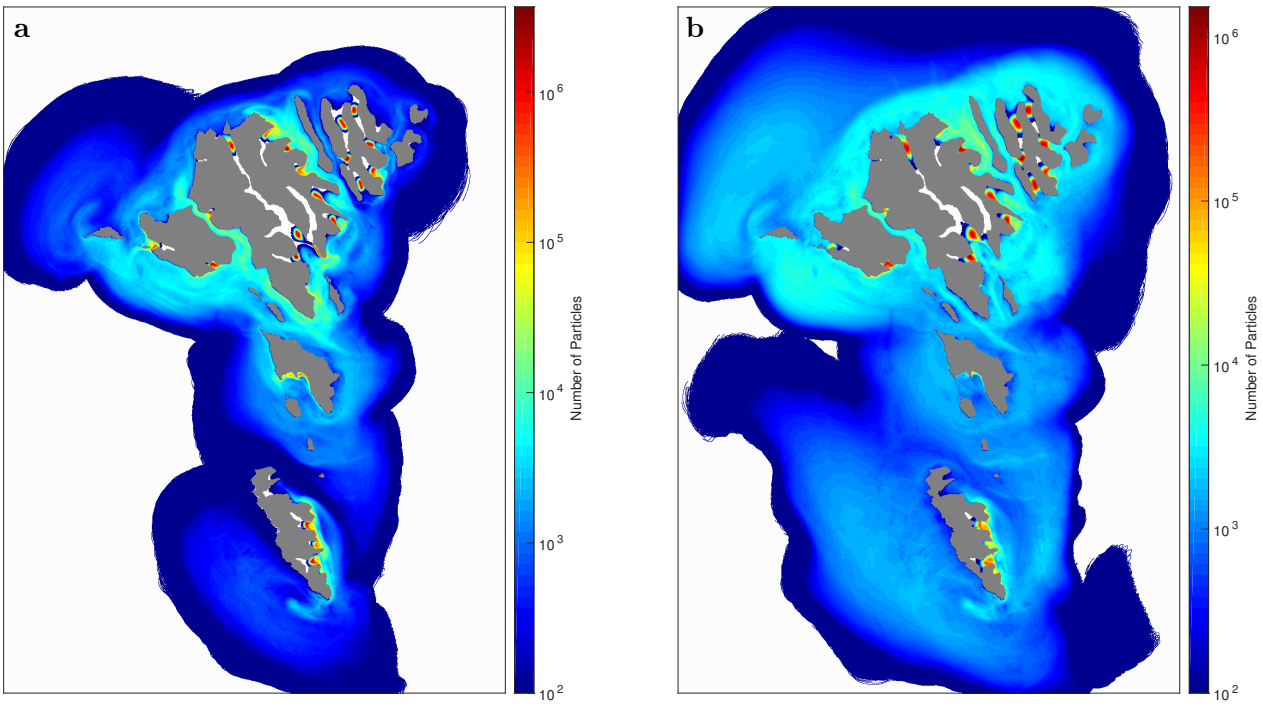

Figure 5: Relative density distribution attained by particles released from all 24 farm sites, by recording the number of particles in each 100x100m grid cell every time step including mortality over the whole 2000 hour simulation. **(a)** and **(b)** shows the number of nauplii and copepodid particles, respectively. Colorbar indicates number of particles on a logarithmic scale.

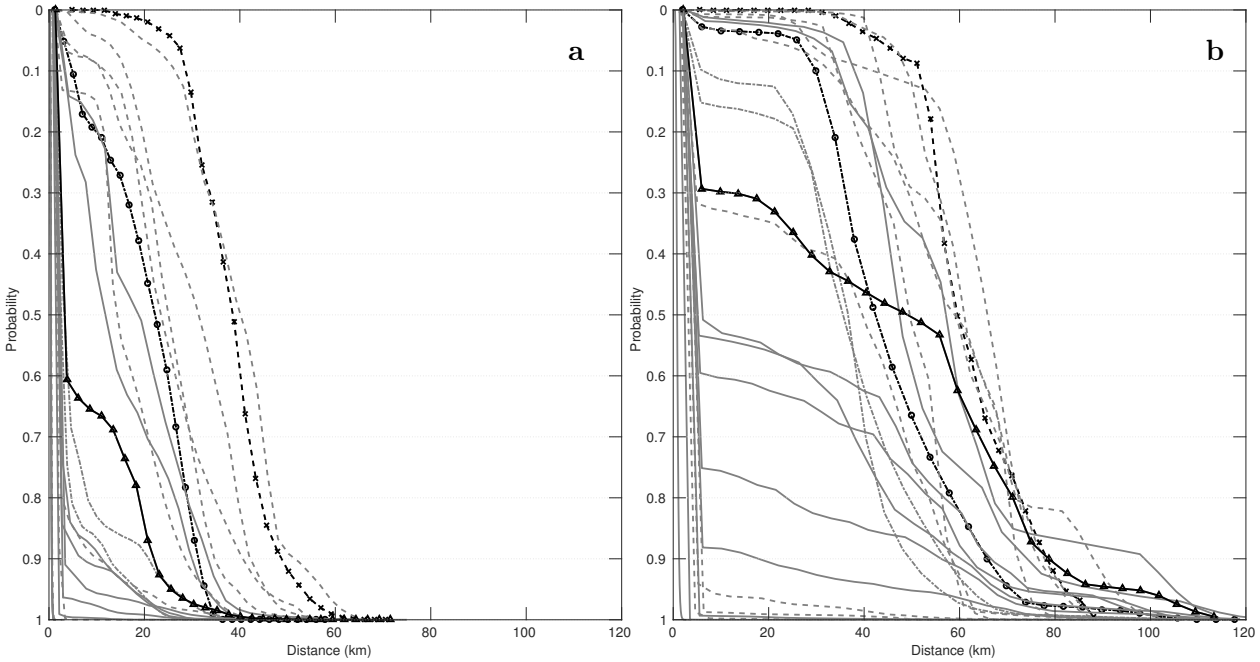

Figure 6: The cumulative frequency of the maximum Euclidean distance attained by particles released from all 24 sites. **(a)** and **(b)** shows the cumulative frequency of the maximum distance, not including the mortality, attained by napulii and copepodid, respectively. Dash-dotted lines are farms 1-3, dashed line are farms 4-13 and solid lines are farms 14-24. As examples, three farms are highlighted: farm2 (dash-dotted line with circle), farm 5 (dashed line with cross), and farm 21 solid line with triangle).

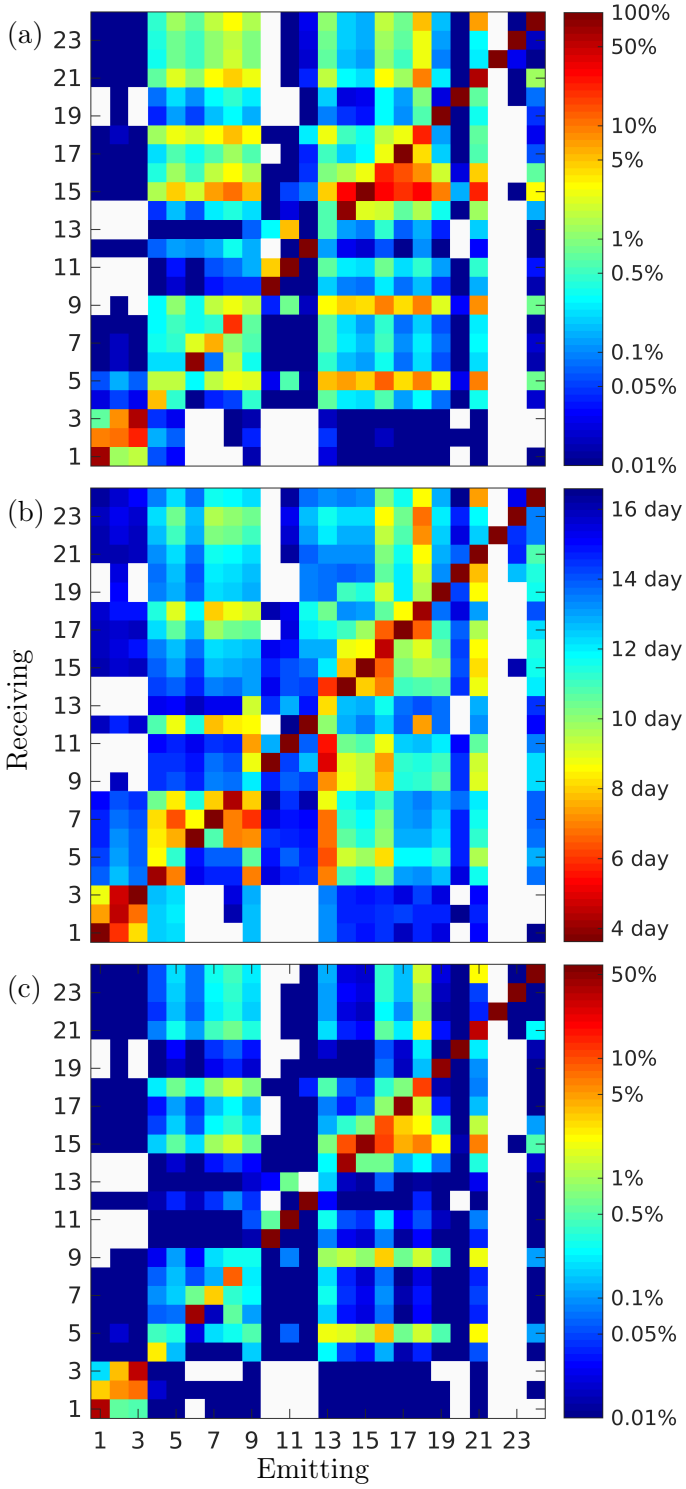

Figure 7: Connectivity matrix's with emitting farms on x-axis and receiving farms on the y-axis. **(a)** Percentage of unique infectious larvae released from one farm site entering any other farm site or its initial release site. **(b)** Mean age of the connections. **(c)** Connectivity including mortality. Colorbar indicates the percentage in **(a)** and **(c)**, scale is logarithmic. Colorbar in **b** indicates the mean age in days. White color indicates that there is no signal.

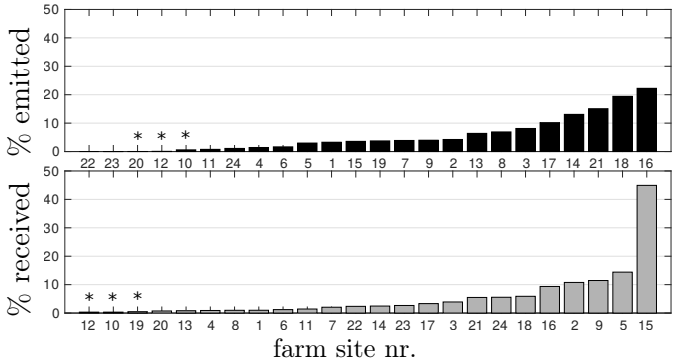

Figure 8: Barplot of % of salmon lice which farms emit (upper panel) and receive (lower panel) to and from other farms accounting for mortality and excluding self-infection."*" indicates the three highly isolated farms. Percentage is normalized with total amount of particles released from one farm.